

IPACK2011-) &% \$

MATERIAL OPTIMIZATION FOR CONCENTRATED SOLAR PHOTOVOLTAIC AND THERMAL CO-GENERATION

Kazuaki Yazawa

University of California Santa Cruz
Santa Cruz, CA, U.S.A.

Ali Shakouri

University of California Santa Cruz
Santa Cruz, CA, U.S.A.

ABSTRACT

We conducted an analytic study of concentrated solar photovoltaic and hot water co-generation based on various solar cell technologies and micro channel heat sinks. By co-optimizing the electricity generation and heat transport in the system, one can minimize the cost of the key materials and compare different tradeoffs as a function of concentration ratio or other parameters. Concentrated solar Photovoltaic (PV) based on multi junction cells can yield around 35-40% efficiency. They are suitable for high photon energy flux and they are already available in the market. However, due to high heat fluxes at large concentrations, such as 100-1000 Suns, heat sinks could be costly in terms of material mass, space, energy for pumping fluid, and system complexity. In addition, since the efficiency of solar cells decreases as the ambient temperature increases, there is a tradeoff between electricity and hot water cogeneration. Similar to our previous analysis of thermoelectric (TE) and hot water co-generation, PV/solar thermal system is also optimized. The results are compared with thermoelectric systems as a function of the concentration ratio. The solar concentrated co-generation system using either PV or TE for direct electricity generation collects more than 80% of solar energy when it is optimized. We calculate the overall cost minima as a function of concentration ratio. Although there are some differences between PV and TE, the optimum concentration ratio for the system is in the range of 100-300 Suns for both.

INTRODUCTION

There is an emergent need for renewable and zero emission energy sources. The Sun is the basis of almost all renewable energies on earth. There are extensive activities in the area of solar photovoltaic (PV) electricity generation as well as in solar thermal hot water systems. The goal is to decrease the production cost (\$/W) and increase the system reliability and lifetime. Conventional fossil fuel based power plants can achieve high efficiencies using co-generation of electricity and hot water. However conventional power plants do not scale well for individual houses or small buildings. There is no doubt that photovoltaic and solar thermal are both well developed and commercialized. However, there is still a big challenge in harvesting energy in specific areas, which turns in to the harvesting energy density. This discussion is most relevant for energy supplies in residential housing. Both electricity and hot water are essential in everyday life applications. We previously reported the energy efficiency of an optimized solar concentrated thermoelectric and hot water system [1]. At the optimum concentration, around 100x, we could harvest 10% of the solar energy as electricity and 70% of the solar energy as heat, for a total of 80%. The thermoelectric device can be designed to match the temperature range with proper choices of temperature dependent materials [2]. This was the advantage we considered in the previous work. However, the conversion efficiency is moderate [3] in comparison to the concentrated solar photovoltaic, for which multi-junction cells are typically used, and efficiency is around 35-40% [4]. Photovoltaic materials are typically temperature dependent and it was reported that the conversion efficiency from the

irradiated photons degrade as absolute temperature increases [5]. So, which technology could work better? Or, are there any specific conditions allowing either one to be optimum? This study will focus on co-optimizing the PV and hot water heat sink. Then we will compare the performance and cost for the different concentration conditions.

SOLAR ENERGY AND CONCENTRATION

Solar irradiation energy has a spectral distribution of energy depending on the wavelength, following Plank's law. By using a band gap of semiconductors, the photon energy is absorbed at the specific spectrum and it excites electrons enough to jump the band gap. Therefore the PV materials are particularly spectrum sensitive. Optical concentration of solar rays is a technique to increase the photon density without making an impact on the spectrum. Multi-junction cells are used to make cells absorb the different light spectrums, to maximize the harvesting of photon energy. This absorbed but not converted spectrum is lost to dissipation due to the insensitive band gap. This is a major loss in photovoltaic devices. In addition, heat generation comes from Joule heating at the internal resistance and parasitic contact resistances. The efficiency of energy conversion of the cutting edge multi-junction PV cells is observed at around 40% while the device is maintained at room temperature [6]. To harvest the rest of the energy dissipated as much as possible, a water cooling heat sink is considered in this model. Not all of the full spectrum of solar irradiation arrives at the ground. It may be scattered or absorbed in the upper atmosphere, so we will take this into account. Radiation angle is another parameter that limits the energy density of solar. However, we could assume that automatic ray tracking [7] could overcome most of this degradation. For a fair comparison, the source density is considered to be the same as thermoelectric and hot water systems. Energy flux E [W/m²] is found as previous work [1] as

$$E = \varepsilon \sigma \left(C f T_{sun}^4 + (1 - C f) T_p^4 - T_h^4 \right) / A_{module} \quad (1)$$

where $f=2.15e-5$, $T_p=288.7K$, $T_{sun}=5762K$, and σ is the Stefan-Boltzmann constant $5.67 \times 10^{-8} \text{W/m}^2\text{K}^4$. The emissivity ε is a spectral characteristic property of the surface [8]. This is reasonable for the typical design of the surface coating of commercialized PV cells. However, we assume a constant number 0.95 in the active spectrum of solar. The concentration ratio C is the design parameter for this case and the A_{module} is the area of the PV cell.

HEAT SINK DESIGN AND PUMP POWER

A heat sink is directly attached underneath a PV cell with same footprint to absorb the dissipation. We could consider a thin dielectric layer and good thermal conductive material on a copper heat sink. There is a significant amount of work on heat sink optimization as described in several studies such as [9] [10] [11]. In this study, a similar model of Yazawa et al. [1] is used. We assume a heat sink where the fluid path is made of parallel channels as shown in Fig. 3. In this figure, the water flows through the channels to a direction perpendicular to the paper plane. A single layer of parallel circular tubes channels are placed with a $\frac{1}{2}$ diameter gap. Therefore the thickness of the heat sink depends on the channel diameter.

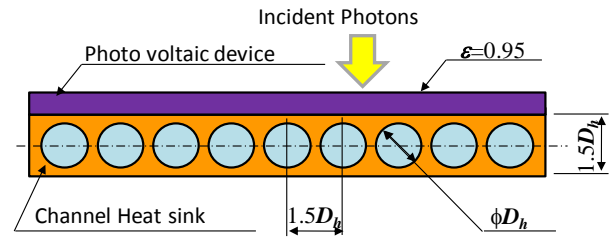


Figure 3. Heat sink attached to TE module

In this section, we will optimize the channel design to minimize the pumping power for a given thermal resistance. From the discussion in Ref. [12], the optimum condition can be found when the convection from the fin surface matches that of the temperature sensitive fluid flow. This is an impedance match between the heat flow from the fin and the fluid reservoir. The impedance match condition is described as

$$U_{BASE} A_{BASE} = 1 / \left(\frac{1}{2\rho C_p G} + \frac{1}{U_{fin} A_{fin}} \right) \quad (2)$$

where the convective surface area is

$$A_{fin} = N\pi D_h L \quad (3)$$

where N is Number of channels, L is length [m] of channel. The heat transfer coefficient at the convective surface is

$$U_{fin} = \frac{Nu\beta_f}{D_h} \quad (4)$$

where Nu is the Nusselt number and β_f is the thermal conductivity [W/mK] of fluid (water). It is adequate to assume a fully developed flow for a long aspect channel

($L \gg D_h$). Thus, the Nusselt number for a fully developed laminar flow for uniform heat flux in a circular tube: 4.634 [13] is applied.

The relation between convective thermal resistance and the sensitive transport thermal resistance is found with referring the intermediate temperature T_m . The point, where the convective heat is transferred, is at the halfway point of the temperature difference, as well as the halfway point of the rise in fluid temperature ($T_{out} - T_{in}$). From this, T_{out} is immediately found to be equal to T_c . Therefore, the flow rate G is found as

$$G = \frac{(q_h - w_{TE})}{\rho C_p (T_c - T_m)} \quad (5)$$

By substituting DL to A_{BASE} and $1/\psi_c$ instead of U_{BASE} in Eq. (24), the diameter of channel is found as

$$D_h = \frac{2\pi Nu \beta_f}{3U_B} \quad (6)$$

From the geometry shown in Fig. 3, the number of channels is found as

$$N = \frac{2D}{3D_h} - 1 \cong \frac{2D}{3D_h} \quad (7)$$

Knowing G , D_h and N , the mean flow velocity in a channel u is found as

$$u = \frac{2G}{N\pi D_h^2} \quad (8)$$

The pressure drop ΔP_{ch} caused by friction loss in the entire internal wall of the channel is determined assuming a fully developed flow, and the pressure loss caused by contraction/expansion is found to be negligible.

$$\Delta P_{ch} = \frac{48\mu L}{D_h^2} u \quad (9)$$

Finally, pumping fluid power is determined by

$$w_{pp} = G\Delta P_{ch} \quad (10)$$

The pumping power is summarized as a function of the heat transfer coefficient U_{BASE} .

$$w_{pp} \cong \frac{10\mu DL^3}{(Nu\beta_f)^3 (\rho C_p)^2} U_B^5 \quad (11)$$

Since electro-mechanical and mechanical-fluid momentum energy conversion losses exist, the efficiency needs to be considered. The overall fluid pump efficiency η_e is picked from off-the-shelf pumps and assumed to be 60%.

$$w_{e-pp} = w_{pp} / \eta_e = 0.6G\Delta P_{ch} \quad (12)$$

The model is based on laminar flow regime. To verify if the model predicts the pumping power correctly, the Reynolds number Re can be used to see if the flow is laminar or if there is transition to turbulence. The criterion for transition to turbulent flow regime in a circular tube is at a Reynolds number of around 2300. Following is the definition of the circular tube based Reynolds number.

$$Re = \frac{\rho u D_h}{\mu} \quad (13)$$

ANALYSIS AND DISCUSSION

An example study for a cutting edge performance of multi-junction PV cells is shown in Figs 4-7. The temperature dependent efficiency $\eta(T)$ is modeled as

$$\eta(T) = \eta_0 - k(T - T_0) \quad (14)$$

where k is the temperature coefficient set to 0.05%/K with considering [6]. We assumed the room temperature efficiency $\eta_0 = 40\%$ at $T_0 = 293^\circ\text{K}$. The efficiency can be considered concentration dependent value. However the impact of temperature and concentration ratio was not clearly separated due to the conjugated phenomena in the device level characterization. Thus, we picked the Eq. (14) as the primary dependency for the efficiency.

Fig. 4 shows the electric and heat output per panel area for the case of water inlet temperature of 60°C . The overall harvesting peak observes 935W/m^2 at $C \sim 140$ and electric power peak observes 357W/m^2 at $C \sim 65$. The ratio of electricity at $C=100$ is 37% of total energy harvesting. Fig. 5 shows the power gain per panel area vs concentration. Slight difference between inlet temperatures is observed. Significant degradation is observed over 100x concentration as Fig. 4. Fig. 6 shows the same power gain but per device area. The optimum concentration is different depending on the base unit. For this metric, the optimum is observed at $C \sim 650$.

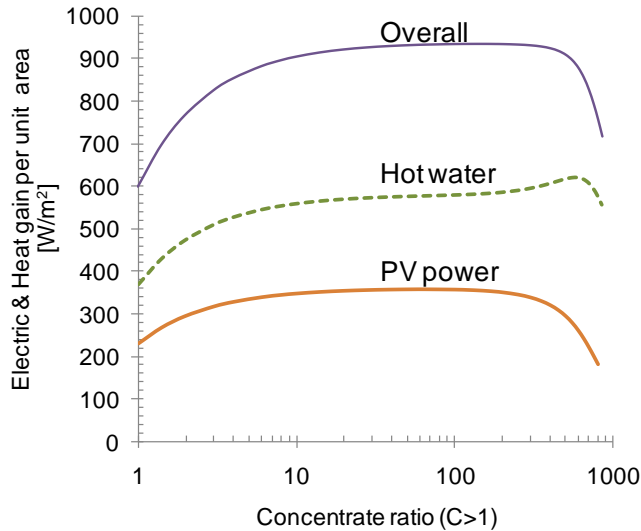


Figure 4. Electric and heat gain per panel (lens footprint) versus concentration ratio for water inlet temperature at 60°C.

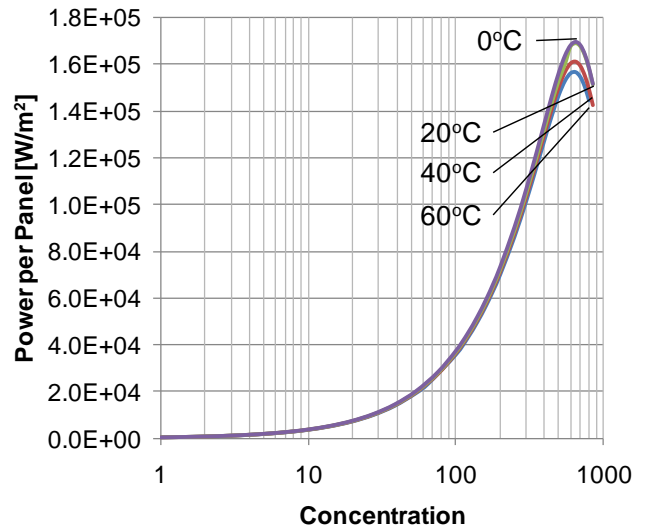


Figure 6. Power gain per device footprint area versus concentration ratio for water inlet temperature at 0°C (magenta), 20°C (green), 40°C (red), and 60°C (blue).

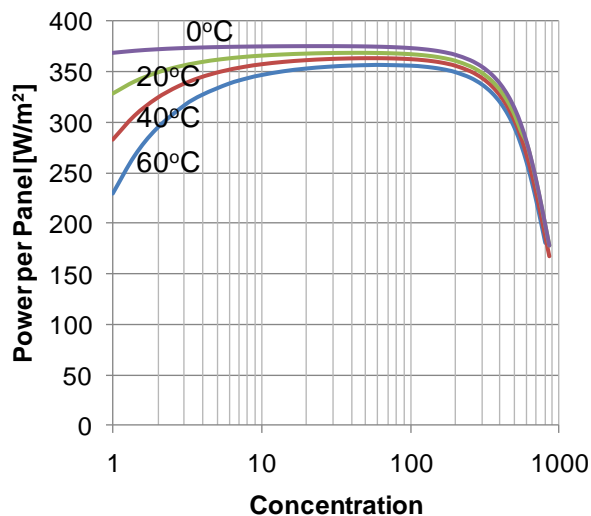


Figure 5. Power gain per panel (lens footprint) versus concentration ratio for various water inlet temperatures.

Fluid dynamic characteristics are shown in Fig. 7. The required pump power is significantly smaller than the generated power for the entire range from $C=1$ to a concentration around 800x. Thus the power loss is not seen in the previous figures. The curves in the figure are drawn based on each individual unit, which is described in the legend. Thus, Y axis does not have specific unit.

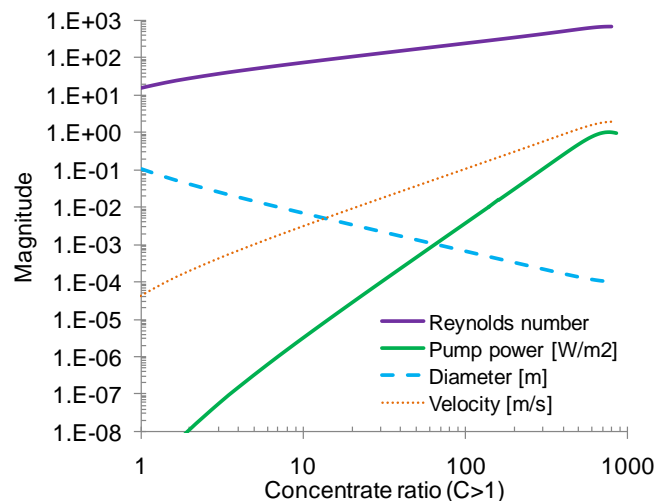


Figure 7. Fluid dynamic characteristics versus concentration ratio for inlet water temperature at 60°C

Fig. 8 shows the efficiency of different conversion efficiency materials with the same rule of temperature dependency as Eq. (14). The solar energy is 985W/m^2 so that the peak efficiency of the multi junction PV observes

94.6% at around 140x.

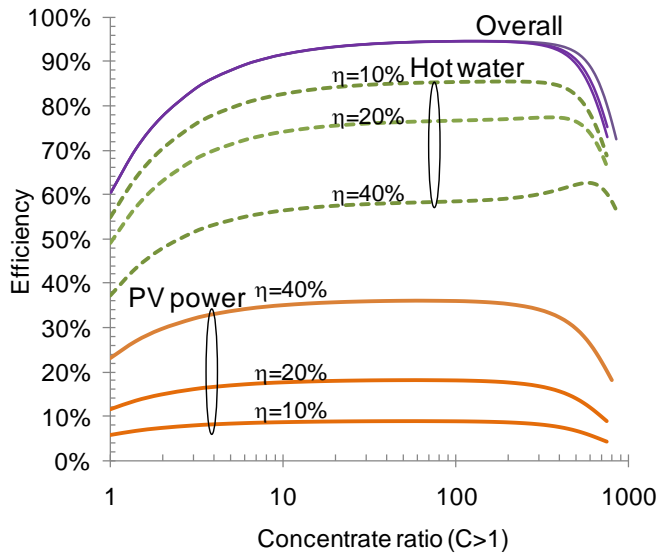


Figure 8. Efficiency of Overall gain, Hot water, and PV power for different PV efficiencies.

COST DISCUSSION

In this section the cost of the system is investigated. Different solar concentration technologies and the scalability challenges of different lenses are not considered. To produce a simple example, a Fresnel lens made of polycarbonate is considered. The thickness of the lens practically depends on the panel size. However, we fix the thickness to contrast the effect of shrinking the photovoltaic device. Here we consider a fixed lens cost per unit area 1m^2 . The cost of the rigid mechanical frame and the tracker is not included and it will be discussed in future publications. The cost of the lens panel is based on material prices in the range of $\$3/\text{kg}$. The heat sink cost is based on copper prices of $\$7.30/\text{kg}$. The cost of thermoelectric materials is more complex, since the specific materials used depend on the temperature range, which is related to the concentration ratio. Since the heat sink model does not consider the mass optimum design, this tends to overestimate the mass especially for smaller heat fluxes which are equivalent to lower concentrations.

A typical unit price of the multi-junction photovoltaic material GaInP/GaAs/Ge is estimated at approximately $\$5000/\text{kg}$. The typical multi-junction PV device has a thickness in the range of $140\mu\text{m}$. For comparison, examine the single crystal silicon with an efficiency of 20% and a thickness of $300\mu\text{m}$, and the copper indium gallium selenide (CIGS) thin film with an efficiency of 10% and a thickness

of $20\mu\text{m}$. The footprint areas of the photovoltaic and the heat sink shrink linearly as the concentration ratio increases. Fig. 10 shows the cost per unit power gain for the system and various devices in respect to the concentration ratio. As we already notice the significant performance drop at over 800x, the figure shows the smaller range only. It is clear that anything less than 10 times the concentration does not lead to better performance. Thus the plot is omitted for the concentration of less than 4x. The cost minimum is observed at different concentration for different devices. Considering electric power only, the minimum cost is observed at $0.25\$/\text{W}$ at around 300x and $0.09\$/\text{W}$ at around 450x for the overall power. Fig. 11 is taken from our previous work [1]. The cost performance, in comparison, yielded a similar minimum cost of around $0.1\$/\text{W}$ and a similar optimum concentration around 300-450x. The cost is comparable to various large scale power generation systems reported in [14]. A slight difference between the two technologies is found in the range of 10-100x concentration. The smaller element coverage F of the element for TE module reduces more the cost, but converges to the same over 100x.

Above cost analysis is intended to find the theoretically minimum. Thus, it should be the end of the learning curve and based on extremely large volume production. Some potential degradation, which means higher cost, would be better considered for the further industrial cost estimation, such as transparency degradation of the optics for years of operation.

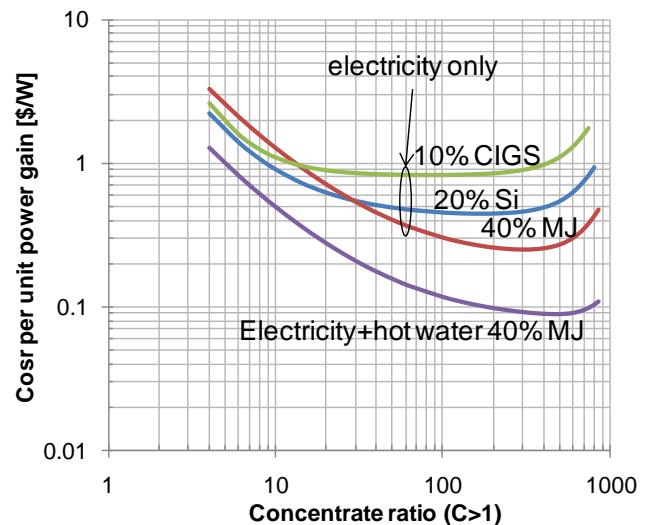


Figure 10. Device and system cost per total output power [\$/W] versus concentration ratio for various photovoltaic $\eta_0=40\%$, 20% , and 10% with $T_{in}=60^\circ\text{C}$ is assumed.

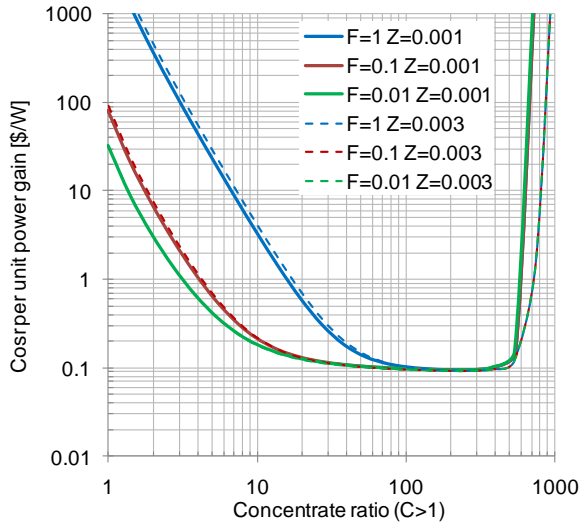


Figure 11. System cost per total output power [\$/W] versus concentration ratio for different TE with fill factors, $T_{in}=60^{\circ}\text{C}$, $Z=0.001$ is assumed[1].

Fig. 12 shows the installation cost of this system. The order of the cost leads to the general sense that cheaper material yield more inexpensive system installations. The interesting region is observed at the concentration over 100x. Most of the cost in this range comes from the lens, and the difference among the material diminishes as the concentration increases. Without considering the mechanical complexity, >100x concentration works more efficiently and costs less. And there is still an option to choose the material for the concentrated solar photovoltaic.

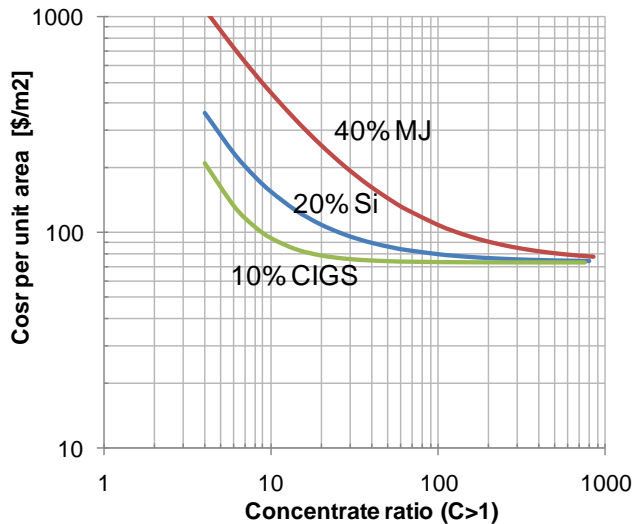


Figure 12. Cost per unit area [\$/m²] of overall system. ‘MJ’ is multi-junction cell, ‘Si’ is single crystal silicon, and ‘CIGS’ is the copper indium gallium selenide.

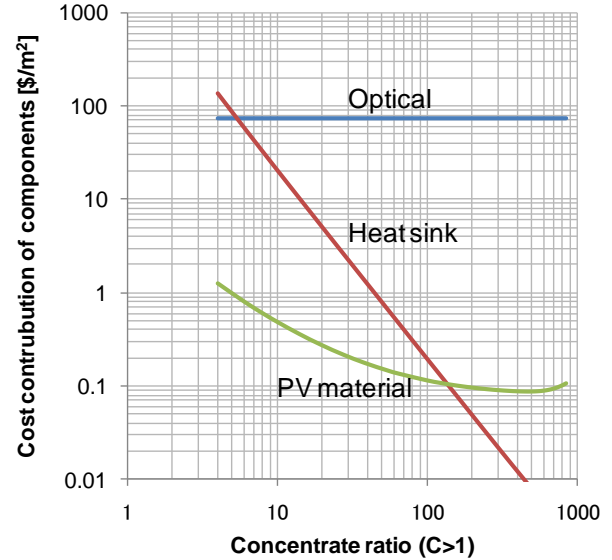


Figure 13. Cost structure versus concentration for the 40% efficiency multi-junction with 60°C water.

CONCLUSIONS

In this paper, we proposed a system for co-generation of electricity and heating for hot water, which are both essential for residential applications. This was based on solar concentrators and photovoltaic devices with hot water microchannel heat sinks. Temperature dependent energy conversion efficiency of the photovoltaic was plugged into the thermodynamic system model. Depending on the concentration, the ratio of the energy to warm up the water changed. The optimum performance of electricity harvesting was found at around 100 Suns concentration for the unit area of the system. Per device footprint area, the peak performance was found at around 600 Suns. For the cost investigation, we considered cutting edge multi-junction PVs designed for concentrated solar as well as plain low cost PV materials. We observed that the smallest cost per output [\$/W] peaked at 300x, but improvements were still significant at concentrations as low as 200x and as high as 400x. We tried to find the cost based on the end of the learning curve and the extremely large volume. Thus, the discussed cost is the theoretically achievable minimum. The multi-junction PV showed the smallest cost within the range of 100-800 Suns. There was no value found for concentration systems in the range of 10 times or smaller. In comparison to the thermoelectric, the optimum concentration was slightly higher and the theoretical power cost minimum limit was at nearly the same range of 0.10\$/W. This result suggests potential and shows the value of further

engineering development for commercialization of either photovoltaic or thermoelectric systems. Since the pumping power penalty was small for the PV system in the optimum output concentration, the combined efficiency including both electricity and heat output showed as high as 94.6% in this theoretical model. And the electricity efficiency is around 1/3 of the overall efficiency at the peak. As a system, the cost per output optimum was found at 100-300 Suns and this result was similar to the thermoelectric systems despite the difference of the mechanisms. These results suggest the PV and TE are the comparable within an order of magnitude for wide range analysis. The technology developments can be considered for the choice of both TE and PV for the concentrated solar power and hot water system.

ACKNOWLEDGMENTS

This work was supported by Center for Energy Efficient Materials funded by the Office of Basic Energy Sciences of the US Department of Energy.

REFERENCES

- [1] K. Yazawa and A. Shakori, System Optimization of Hot Water Concentrated Solar Thermoelectric Generation, Proceedings of ThETA 3 conference, 2010.
- [2] C.J. Vineis, A. Shakouri, A. Majumdar, M.G. Kanatzidis, "Nanostructured Thermoelectrics: Big Efficiency Gains from Small Features", *Advanced Materials*, Vol. 22, pp. 3970–3980, 2010.
- [3] C. Vining, "An inconvenient truth about thermoelectrics", *Nature Materials* 8, pp83–85, 2009.
- [4] R. McConnell and M. Symko-Davies, "Multijunction Photovoltaic Technologies for HighPerformance Concentrators", the 2006 IEEE 4th World Conference on Photovoltaic Energy Conversion (WCPEC-4), 2006.
- [5] G. A. Landis, "High-Temperature Solar Cell Development", NASA report NASA/CP—2005-213431, pp 241-247, 2005
- [6] G. S. Kinsey, P. Hebert, K. E. Barbour, D. D. Krut, H. L. Cotal and R. A. Sherif, "Concentrator Multijunction Solar Cell Characteristics Under Variable Intensity and Temperature", *Progress In Photovoltaics: Research and Applications*, Issue 16, pp503–508, 2008
- [7] H.A. Zondag, "Flat-plate PV-Thermal collectors and systems: A review", *Renewable and Sustainable Energy Reviews*, Volume 12, Issue 4, pp891-959, 2008
- [8] D. Labuhn and S. Kabelac, "The Spectral Directional Emissivity of Photovoltaic Surfaces", *International Journal of Thermophysics*, Vol. 22, No. 5, pp 1577-1592, 2001
- [9] Y. Murakami, Y. et al., "Parametric Optimization of Multichanneled Heat Sinks for VLSI Chip Cooling", *IEEE Transaction on Components and Packaging Technologies*, Vol. 24, No. 1, pp2-9, 2001
- [10] P. Teertstra et al., "Analytic Modeling of Forced Convection in Slotted Plate Fin Heat Sinks", *Proceedings of 1999 ASME International Mechanical Engineering Congress and Exposition*, HTD-Vol. 364-1, Vol.1, pp3-11, 1999.
- [11] M. Iyengar et al., "Least-Energy Optimization of Air-Cooled Heat Sinks for Sustainable Development", *IEEE CPT Transactions*, Vol. 26, No.1, pp16-25, 2003.
- [12] K. Yazawa et al., "Thermofluid Design of Energy Efficient and Compact Heat", *Proceedings of 2003 International Electronic Packaging Technical Conference and Exhibition*, IPACK2003-35242, 2003.
- [13] K.K. Shah and M.S. Bhatti, "Laminar Convection Heat Transfer in Ducts", *Handbook of Single Phase Convective Heat Transfer*, 1987.
- [14] National Renewable Energy Laboratory, "Energy Technology Cost and Performance Data", http://www.nrel.gov/analysis/tech_costs.html, 2010.